[Frontiers in Bioscience 11, 1147-1157, January 1, 2006]

A redox active and electrochemiluminescent threading bis-intercalator and its applications in DNA assays

Hong Xie [1], Natalia C. Tansil [1,2] and Zhiqiang Gao [1,2]

[1] Institute of Bioengineering and Nanotechnology, 31 Biopolis Way, Singapore 138669, [2] School of Materials Science and Engineering, Nanyang Technological University, Singapore 639798

TABLE OF CONTENTS

1. ABSTRACT

A redox active and electrochemiluminescent (ECL) threading bis-intercalator, consisting of two N,N'-bis(3-propyl-imidazole)-1,4,5,8-naphthalene diimides (PIND) linked by a $Ru(dmbpy)_2^{2+}$ (dmbpy = 4,4'-dimethyl-2,2'-bipyridine) complex (PIND-Ru-PIND), was synthesized for the first time. Its optical, electrochemical, and ECL properties were studied. UV-vis spectrophotometric measurements indicated that the two PIND groups bind to the double-stranded DNA (ds-DNA) in a threading intercalation mode, while the $Ru(dmbpy)_2^{2+}$ reinforces the intercalation via electrostatic interaction with ds-DNA. An ECL DNA biosensor was fabricated using PIND-Ru-PIND. A 2000-fold sensitivity enhancement over direct voltammetry was obtained, making this an ultrasensitive system for ECL detection of DNA. Under optimized conditions, the biosensor allowed the detection of a target DNA in the range of 0.70– 400 pM with a detection limit of 400 fM.

2. INTRODUCTION

In recent years considerable interest has been focused on the development of ultrasensitive DNA biosensors following the completion of Human Genome Project. These biosensors have a wide variety of potential applications that range from genotyping to molecular diagnostics (1-3). Due to insufficient sensitivities of fluorescence-based methods, other transduction techniques, such as autoradiographic (4), electrochemical (1,2), chemiluminescent (5), and ECL methods (6) have therefore been proposed for ultrasensitive detection of DNA hybridization events. Among them, ECL has been demonstrated in the commercialized products as one of the most sensitive techniques to date. ECL is the process of generating excited states in a photoactive molecule at an electrode surface, leading to luminescence upon return to the ground state. One compound that has been extensively studied is $Ru(bpy)_3^{2+}$ (7-9). ECL of $Ru(bpy)_3^{2+}$ was reported by Bard some thirty years ago (10). Because of its

low-lying metal-to-ligand charge-transfer (MLCT) excited states (7), high emission quantum yields (~4.2% in H_2O) (8,9) and long excited-state lifetimes (~600 ns), the well-known $Ru(bpy)_3^{2+}$/tri-n-propylamine (TPA) system is usually adopted in analytical applications.

ECL as a DNA detection technique has the potential to match or exceed the sensitivity of autoradiography (6). The key to the ultrahigh sensitivity of ECL lies in its ultralow background noise, which is a direct consequence of having two different forms of energy for analytical signal generation and detection. Unlike fluorescence-based techniques, ECL does not involve an excitation light source and it theoretically produces a "zero" background. A promising approach toward the enhancement of the ECL signal is to build up multiple ECL tags on a single ds-DNA chain. This strategy has the advantage of providing multiple redox sites, greatly increasing the number of charge recombination events per target DNA molecule, and thereby enhancing the intensity of analytical signal and lowering the detection limit. Two fundamental issues that need to be addressed in the development of multiple ECL tag system are (i) accessibility of ECL redox sites to the electrode and to active TPA species and (ii) electronic independence of the redox sites to avoid intramolecular energy transfer from the excited site to the lowest-lying unoccupied molecular orbital of an acceptance site. As demonstrated by Bard *et al.*, as little as 1.0 fM DNA is detected when a $Ru(bpy)_3^{2+}$ doped polystyrene microbead (Ru-PMB) is used as an ECL tag (6). An oligonucleotide capture probe (CP) is first immobilized on a magnetic bead via biotin-avidin conjugation, and the complementary target DNA, labeled with a Ru-PB, hybridizes with the CP. The hybridized Ru-PB is then magnetically separated and transferred into acetonitrile where $Ru(bpy)_3^{2+}$ is released and quantified electrochemiluminescently. The Ru-PMB is beneficial both for target DNA immobilization and for amplifying ECL signal (6).

The use of an electroactive DNA intercalator as a hybridization indicator negates the need for labeling the target DNA as commonly required in conventional DNA detection techniques (6, 11-14). Tedious labeling procedures and expensive equipment are not involved. New intercalators, offering better discrimination between single-stranded DNA (ss-DNA) and ds-DNA are being developed for achieving greater signal/noise ratio. Our group has been interested in using redox active threading intercalators to tag DNA and develop ultrasensitive DNA detection systems. In a previous report, we described the synthesis and analytical application of a redox active threading intercalator (15). A much better selectivity and a higher stability are expected with a properly designed bis-intercalator. Recently, Rusling and co-workers have reported that ECL signals can be generated in a DNA-$[Ru(bpy)_2PVP]$ bilayer (16). Thus, it is expected that a monomeric compound containing a $Ru(dmbpy)_2(Im)_2$ (Im = imidazole) unit could also be electrochemiluminescent. In addition, the photoefficiency might be enhanced by utilizing surface-confined intercalator of high local concentration of electrochemiluminescence reaction centers and electrochemical recycling mechanism at the electrode surface. The marriage of a highly selective bis-intercalator and ECL will provide a generic platform for ultrasensitive non-labeling detection of DNA.

We report here the synthesis, characterization and analytical application of a redox active and ECL DNA threading intercalator in ultrasensitive DNA biosensors. The $Ru(dmbpy)_2$ complex was sandwiched between two PINDs through coordinative bonds with the two imidazole groups at their termini, forming the PIND-Ru-PIND compound. The intercalated PIND-Ru-PIND exhibited reversible electron-transfer and strong ECL in the presence of TPA. The proposed ECL procedure has a number of advantages: (i) simplicity of non-labeling process, (ii) high sensitivity, (iii) high selectivity, and (iv) high compatibility with microfabrication and multiplexing.

3. EXPERIMENTAL SECTION

3.1. Reagents

1(3-aminopropyl)-imidazole (AI, 98%,) and 1,4,5,8-naphthalene tetracarboxylic dianhydride (NTD, >95%) were purchased from Sigma-Aldrich (St Louis, MO, USA). $Ru(dmbpy)_2Cl_2$ (99%) was synthesized from $RuCl_3$ and dmbpy following the procedure proposed by Lay (17). All other reagents were obtained from Sigma-Aldrich and used without further purification. Capture probes used in this work were custom-made by Alpha-DNA (Montreal, Canada) and all other oligonucleotides were custom-made by 1st Base Pte Ltd (Singapore). Oligonucleotide sequences used in the biosensors were as follows: 5'-CAT TCC GTA GAA TCC AGG GAA GCG TGT CAC-3' (Target DNA), 5'-HS-$(CH_2)_6$-T_6 GTG ACA CGC TTC CCT GGA TTC-3'(capture probe), 5'-CAT TCC GTA GAA TCC AGG GA**T** GCG TGT CAC-3' (one-base-mismatched), 5'-HS-$(CH_2)_6$-T_6-CCT CTC GCG AGT CAA CAG AAT-3' (control). A 10 mM Tris-HCl–1.0 mM EDTA–0.10 M NaCl buffer solution (TE) was used as hybridization buffer.

3.2. Apparatus

Electrochemical experiments were carried out using a CH Instruments model 660A electrochemical workstation (CH Instruments, Austin, TX). A conventional three-electrode system, consisting of a 3.0-mm-diameter gold working electrode, a non-leak Ag/AgCl (3.0 M NaCl) reference electrode (Cypress Systems, Lawrence, KS), and a platinum wire counter electrode, was used in all electrochemical measurements. To avoid the spreading of the sample droplet beyond the 3.0-mm diameter working area, a patterned hydrophobic film was applied to the gold electrode after the immobilization of the CP. All potentials reported in this work were referred to the Ag/AgCl electrode. UV-visible spectra were recorded on a V-570 UV/VIS/NIR spectrophotometer (JASCO Corp., Japan). Mass spectrometric experiments were performed with a Finnigan/MAT LCQ Mass Spectrometer (ThermoFinnigan, San Jose, CA).

Measurements of ECL were performed with a Fluorolog®-3 spectrofluorometer (Jobin Yvon Inc, Edison, NJ) in conjunction with a 660A electrochemical workstation. The three-electrode system consisted of a gold

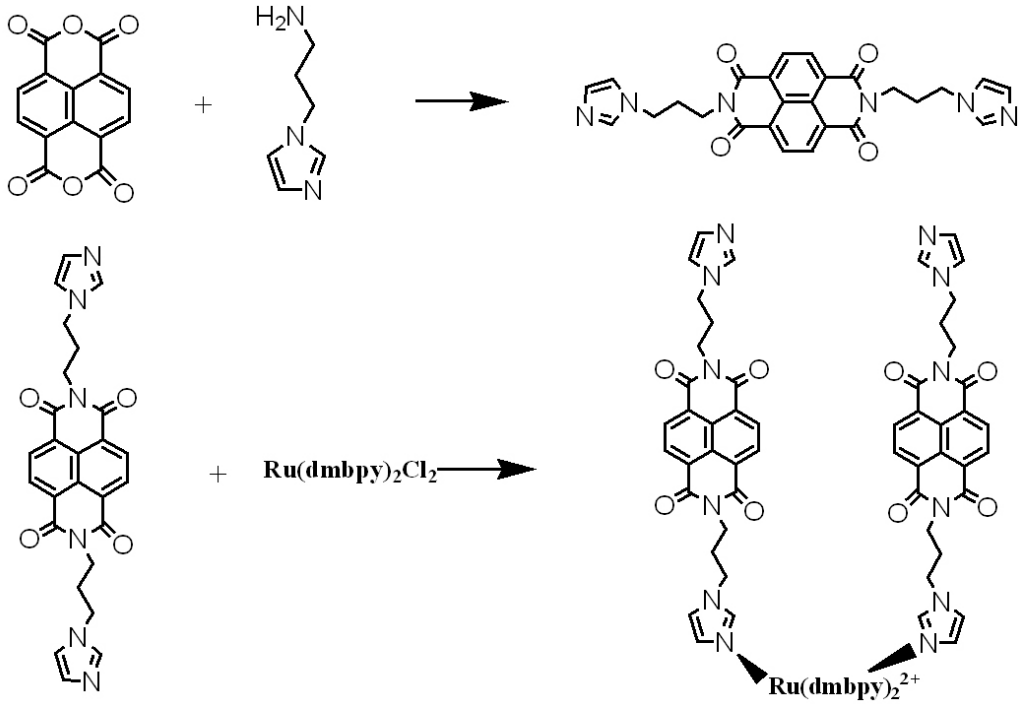

Figure 1. Synthetic scheme of PIND-Ru-PIND.

working electrode, a non-leak Ag/AgCl reference electrode, and a platinum foil counter electrode. The three electrodes were hosted in a standard 1.0-cm fluorescence cuvette and arranged in such a way that the working electrode faces the emission window and the other two electrodes are behind the working electrode. All potentials reported in this work were referred to the Ag/AgCl electrode. All experiments were carried out at room temperature, unless otherwise stated.

3.3. Synthesis of PIND-Ru-PIND

The synthesis of PIND-Ru-PIND is outlined in Figure 1. PIND was prepared following a general procedure for the synthesis of diimide (18,19). Briefly, to a magnetically stirred mixture of 3.0 ml of AI and 3.0 ml of tetrahydrofuran was slowly added 0.30 g of NTD. The rate of addition was controlled so that there was little clogging. The reaction mixture was refluxed for 12 h and then cooled to room temperature. Next, it was dispersed in 10 ml of acetone/water (3/1) mixture and poured into 500 ml of rapidly stirred anhydrous ether to precipitate the compound. The precipitate was collected by suction filtration through a fine fritted funnel and washed briefly with ethanol. The product was purified by running it through a silica gel column using ethanol/chloroform (1/1) as the eluent and dried under vacuum at 40ºC overnight to give 0.36 g of yellow crystals (yield 65%). 1H NMR (300 MHz $CDCl_3$) δ 8.76 (4H), 7.54 (2H), 7.26 (4H), 4.27 (4H), 4.12(4H), 2.31 (4H) and 1.83 (2H). Reverse-phase HPLC–MS tests showed that the desired compound has been successfully synthesized and its purity was >99%, as indicated by a single elution peak at 1.68 min and an m/z of 483.3 (Figure 2).

PIND-Ru-PIND was synthesized in a single-step double ligand-exchange reaction. To a solution of $Ru(dmbpy)_2Cl_2$ (0.20 mmol) in 8.0 ml fresh-distilled ethylene glycol was added 0.50 mmol PIND and the resulting mixture was stirred for 10 min before refluxing. The course of the ligand-exchange reaction was followed by cyclic voltammetry. The orange reaction mixture was then poured slowly into 500 ml of rapidly stirred anhydrous ether. The precipitate was collected by suction filtration through a fine fritted funnel. The crude product was dissolved in 8.0–10 ml of water and was extracted twice with chloroform. The precipitate was further purified by crystallization from ethanol giving the pure product in 80% yield. The product showed a single pair of reversible redox waves at a gold electrode with an $E_{1/2}$ of 0.68 V in aqueous solution. To ensure a complete double ligand-exchange, a slight excess of PIND (20–25%) is required.

3.4. Immobilization of CP on gold electrode

The preparation and pretreatment of gold electrodes were as previously described (20). Briefly, prior to capture probe adsorption, a gold electrode was exposed to oxygen plasma for 5-10 min and then immediately immersed in absolute ethanol for 20 min to reduce the oxide layer. A CP monolayer was adsorbed by immersing the gold electrode in a 20 mM phosphate buffer (pH 7.4) solution of 100 µg/ml CP for 16–24 h. After adsorption, the electrode was copiously rinsed with and soaked in the phosphate buffer for 20 min, rinsed again, and blown dry with a stream of air. The surface density of CP, assessed electrochemically by the use of cationic redox probe according to the procedure proposed by Steel (21), was found to be in the range of $1.15–1.35x10^{-11}$ mol/cm^2. To

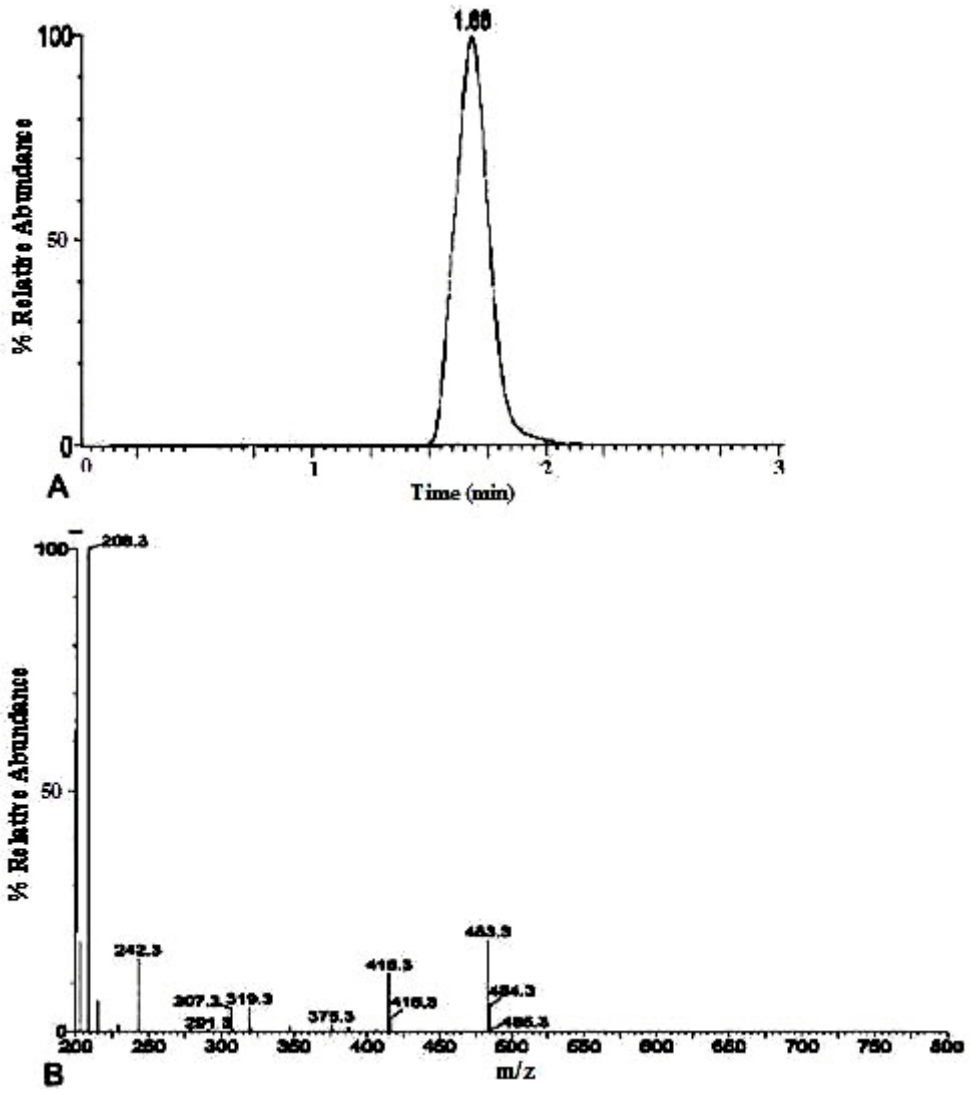

Figure 2. A. Reverse-phase HPLC results of purified PIND. C18 column, Eluent: H_2O. B ESI-MS spectrum of PIND.

minimize non-DNA related PIND-Ru-PIND uptake and improve the quality and stability of the CP monolayer, the CP-coated gold electrode was immersed in an ethanolic solution of 2.0 mg/ml 1-mercaptododecane (MD) for 4–6 h. Unreacted MD molecules were rinsed off and the electrode was washed by immersion in a stirred ethanol for 10 min followed by thorough rinsing with ethanol and water. The electrode was ready after air-dry.

3.5. Hybridization and detection

The hybridization of a target DNA and its ECL detection were carried out in three steps. First, the CP coated electrode was placed in a moisture saturated environmental chamber maintained at 60ºC. A 5.0 µl aliquot of hybridization solution containing the target DNA was uniformly spread onto the electrode (low stringency, 27ºC below the salt-adjusted melting temperature). It was then rinsed thoroughly with a blank hybridization solution at 60ºC after 30 min of hybridization and incubated at 25ºC for 10 min with a 5.0 µl aliquot of 100 µg/ml of PIND-Ru-PIND in the hybridization solution. PIND-Ru-PIND was attached to the hybridized target DNA via threading intercalation. It was then thoroughly rinsed with NaCl-saturated pH 7.0 0.10 M phosphate buffer. ECL was measured at 1.0 V in TPA saturated 0.10 M phosphate buffer (pH 7.0).

4. RESULTS AND DISCUSSION

4.1. Formation of PIND-Ru-PIND

The formation of the redox active PIND-Ru-PIND bis-intercalator can be conveniently monitored by cyclic voltammetry. During reflux in ethylene glycol, cyclic voltammetric tests were conducted every 5 min. Figure 3 shows three typical voltammograms obtained in the first 30 min. Before adding PIND to $Ru(dmpy)_2Cl_2$, one pair of reversible voltammetric peaks centered at 0.29 V were obtained, corresponding to the well-known redox

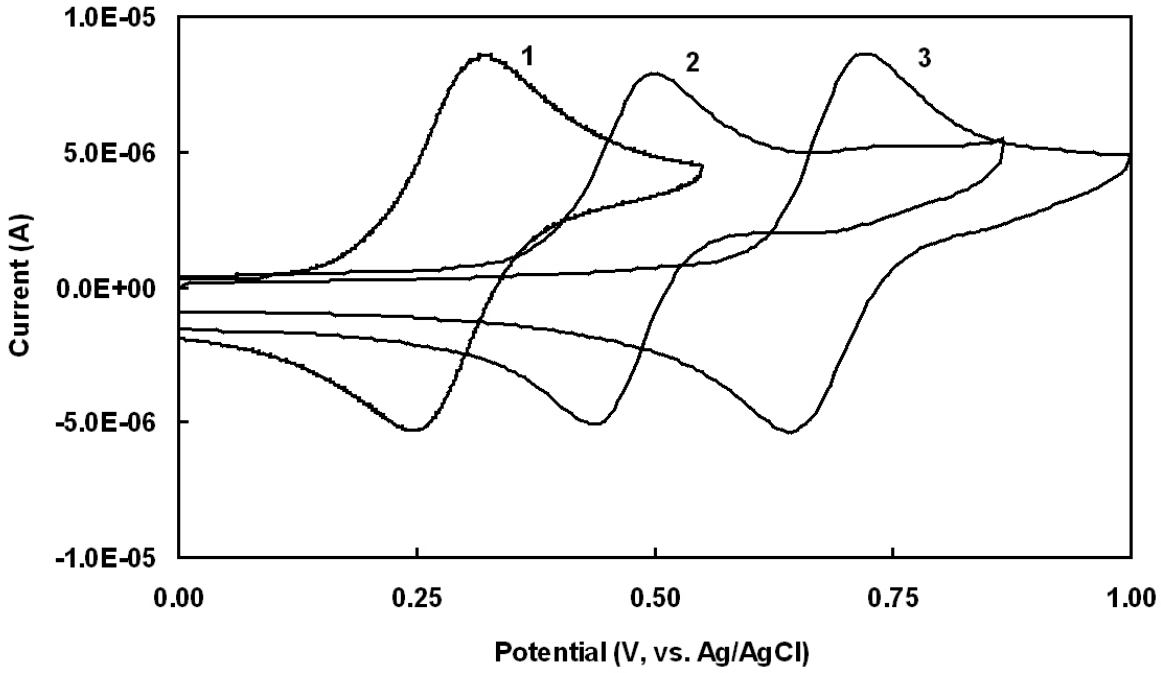

Figure 3. Cyclic voltammograms of $Ru(dmbpy)_2Cl_2$ after (1) 0, (2) 10 and (3) 30 min of refluxing with PIND in ethylene glycol. Supporting electrolyte pH 7.0 0.10 M phosphate buffer, potential scan rate 100 mV/s.

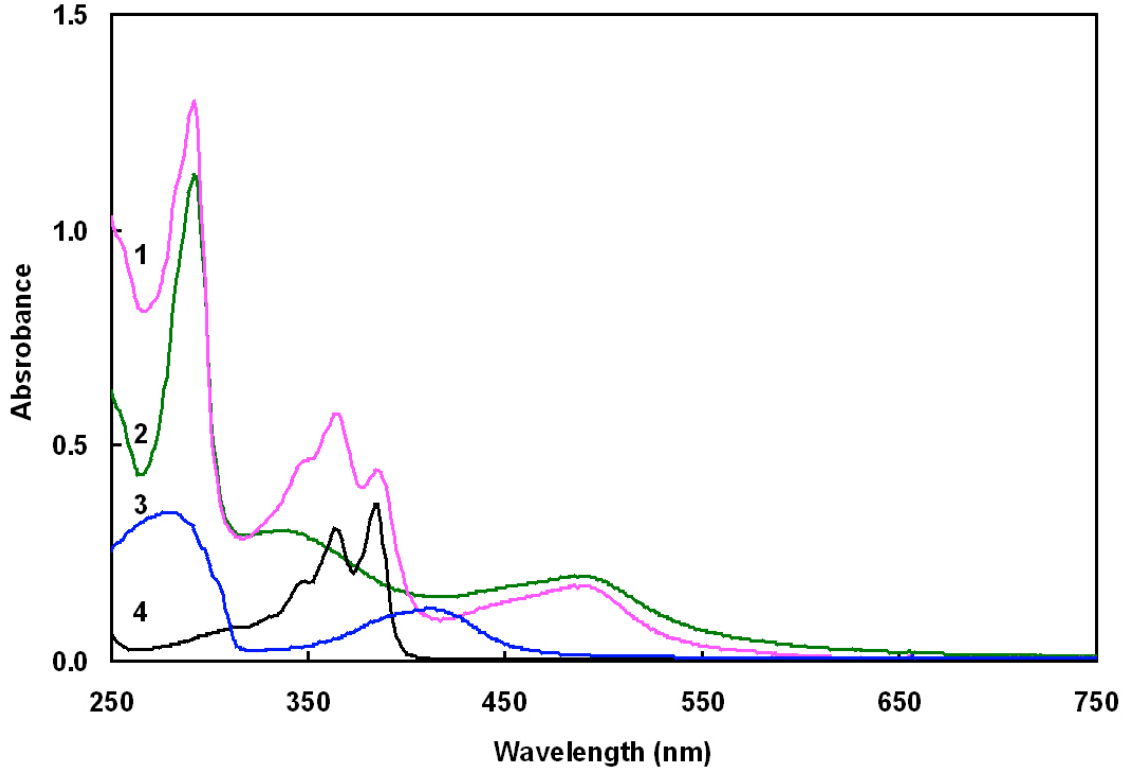

Figure 4. UV-vis absorption spectra of (1) 25 μM PIND-Ru-PIND, (2) 25 μM $Ru(dmbpy)_2(Im)_2$, (3) 25 μM $Ru(dmbpy)Cl_2$, and (4) 50 μM PIND in ethanol.

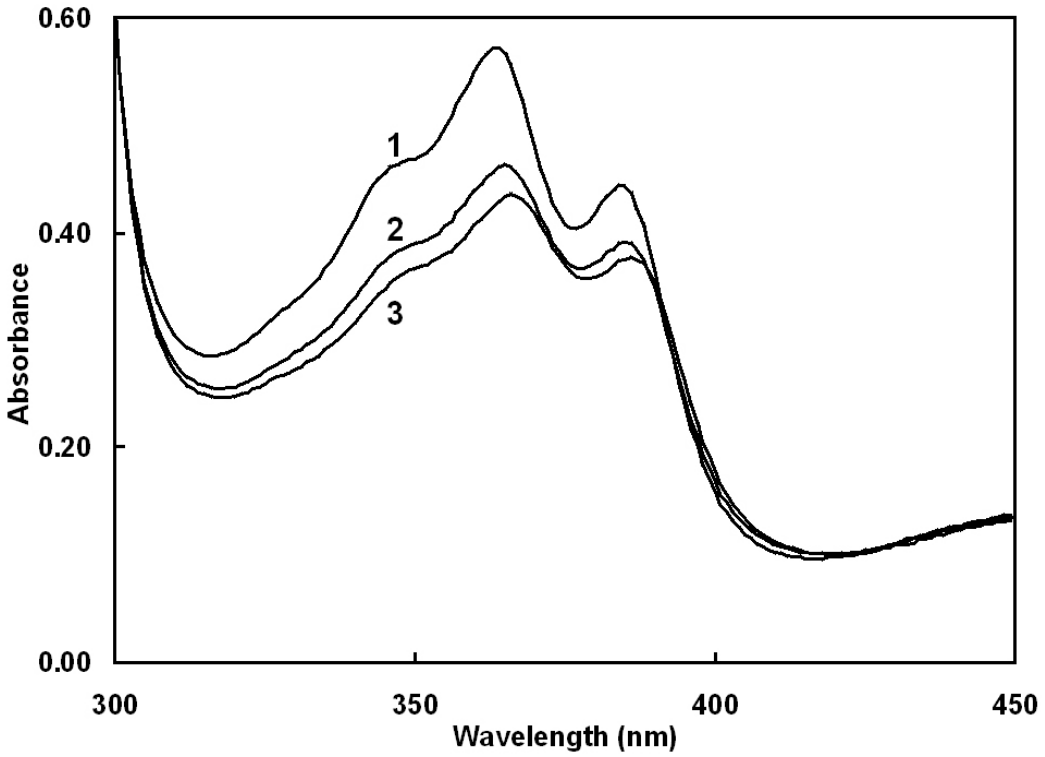

Figure 5. UV-vis absorption spectra of 20 μM PIND-Ru-PIND in 0.10 M pH 7.0 phosphate buffer as a function of increasing concentration of salmon sperm DNA (in base pair) of (1) 0, (2) 40 and (3) 100 μM.

process of $Ru(dmbpy)_2Cl_2$. After only 10 min of refluxing, the voltammetric peaks of $Ru(dmbpy)_2Cl_2$ disappeared completely and two new pair of voltammetric peaks appeared at 0.49 and 0.68 V, indicating the formation of PIND-Ru and PIND-Ru-PIND, respectively (Figure 3 trace 1 and 2). Both electron transfer processes are clearly resolved and have all the characteristics of reversible processes, except the slightly larger peak-to-peak potential separations, that are mainly due to a higher iR drop of the reaction medium. The intensities of the voltammetric peaks at 0.68 V increased gradually with reaction time. Simultaneously, those at 0.48 V diminished gradually. Voltammetric tests of the reaction mixture after 30 min refluxing showed only one pair of voltammetric peaks (Figure 3 trace 3) indicating the completion of the double-ligand exchange process.

UV-vis absorption spectra of the starting materials, a $Ru(dmbpy)_2(Im)_2$ model compound and PIND-Ru-PIND are depicted in Figure 4. UV-vis spectrum of PIND-Ru-PIND (Figure 4 trace 1) is similar to that of $Ru(dmbpy)_3$–naphthalene diimide compound (22-24). It exhibits intense absorption band in the UV region due to intraligand (IL)$\delta \rightarrow \delta^*$(dmbpy) transitions and followed by a broad absorption band in the visible region (400–600 nm) due to spin allowed Ru(dπ)→ dmbpy (π*) MLCT transition (29). The absorption peaks at 380 and 361 nm are mainly due to π→π* transition in PIND with some contribution from underlying MLCT absorbance. The absorption maximum of PIND-Ru-PIND is red-shifted with respect to $Ru(dmbpy)_2Cl_2$, from 415 to 495 nm (Figure 4 trace 3). The same changes were also observed in the spectrum of the model compound $Ru(dmbpy)_2(Im)_2$ as compared to $Ru(dmbpy)_2Cl_2$ (Figure 4 trace 2). This is likely a direct consequence of the ligand exchange which results in two types of MLCT transitions within the ruthenium complex: Ru*→dmbpy, and Ru*→AI. The imidazole groups of PIND are conjugated, resulting in a lower π* level for this ligand relative to the chloride of the complex. Moreover, the spectrum of PIND-Ru-PIND is a composite of the absorption spectra from both the PIND moiety and the $Ru(dmbpy)_2(Im)_2$ complex (Figure 4 traces 1, 2 and 4). A simple overlay of $Ru(dmbpy)_2(Im)_2$ and PIND generated a spectrum which is almost identical to that of PIND-Ru-PIND, confirming the formation of PIND-Ru-PIND.

Although we concluded from UV-vis spectrophotometric and electrochemical evidence that the coupling between PIND and $Ru(dmbpy)_2Cl_2$ results in a coordinative linkage and two PIND molecules are grafted onto $Ru(dmbpy)_2$, a more direct proof of the formation of PIND-Ru-PIND was necessary. Thus we conducted a series of mass spectrometric tests on PIND-Ru-PIND using electron–spray ionization mass spectrometry (ESI–MS). Predominant peaks were found at m/z 717, 483, 478, and 242, corresponding to $(PIND\text{-}Ru\text{-}PIND)^{2+}/2$, $(PIND+H^+)$, $(PIND\text{-}Ru\text{-}PIND+H^+)^{3+}/3$, and $(PIND+2H^+)/2$ respectively, which are in good agreement with the molecular weights of the desired compounds. Since mono-grafted $Ru(dmbpy)_2$ was not observed in the ESI–MS spectrum, we can rule out any incomplete grafting of $Ru(dmbpy)_2$.

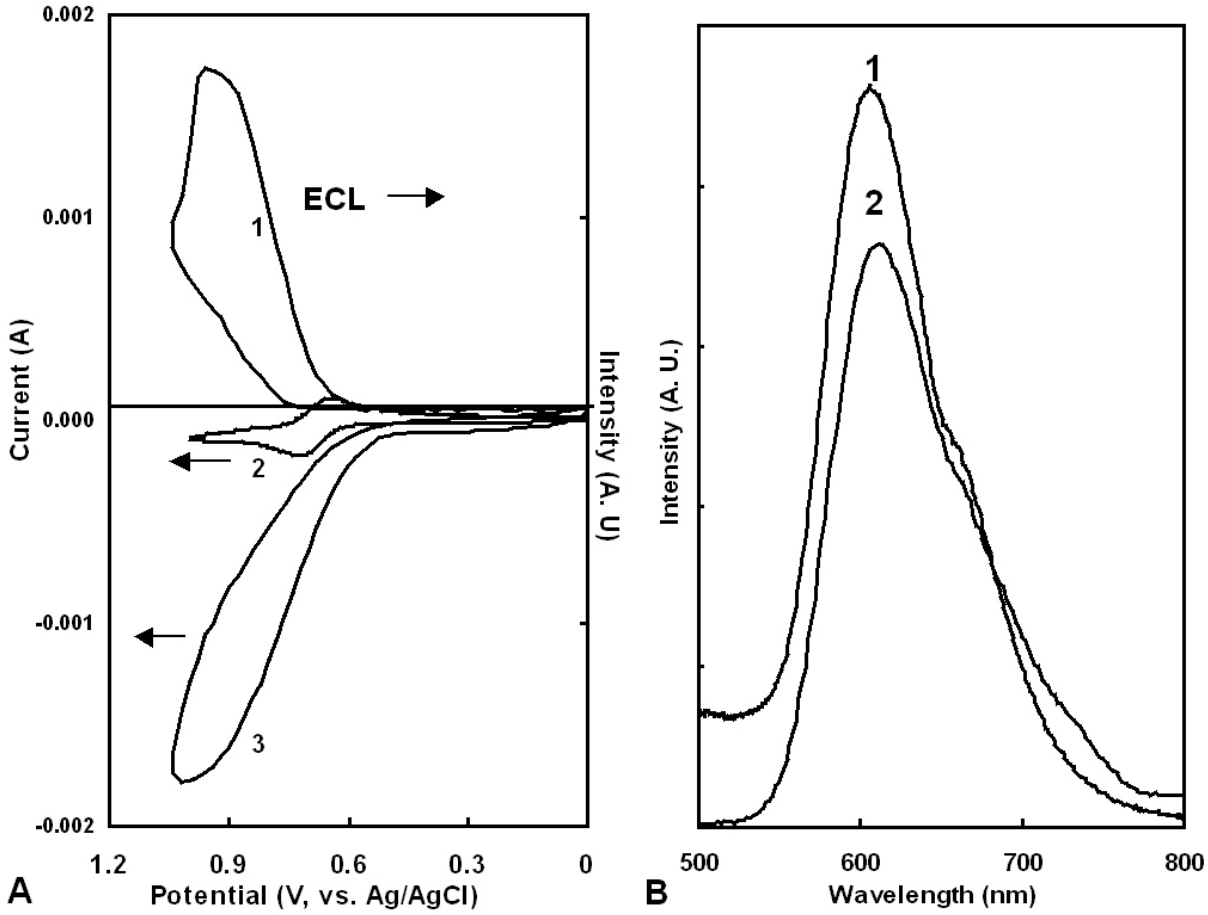

Figure 6. A. (1) ECL intensity at 610 nm versus potential profiles, cyclic voltammogram of (2) 5.0 μM PIND-Ru-PIND in a pH 7.0 0.10 M phosphate buffer, and (3) a TPA saturated pH 7.0 0.10 M phosphate buffer containing 5.0 μM PIND-Ru-PIND. Potential scan rate 20 mV/s. For clarity, the voltammogram of PIND-Ru-PIND was scaled up 50 times. B. (1) Photoluminescence spectrum of PIND-Ru-PIND (430 nm illumination) in a pH 7.0 0.10 M phosphate buffer and (2) ECL spectrum of PIND-Ru-PIND in a TPA saturated pH 7.0 0.10 M phosphate buffer containing 5.0μM PIND-Ru-PIND.

4.2. Electrochemical properties of PIND-Ru-PIND

As illustrated in trace 3 in Figure 3, PIND-Ru-PIND behaved exactly as expected for a highly reversible Ru(II)/Ru(III) redox couple in an aqueous solution. Little change was observed after numerous repetitive potential cycling between 0.0 and +1.0 V, revealing a good stability of PIND-Ru-PIND. At slow scan rates, <1.0 V mV/s, a typical diffusion-controlled voltammogram was recorded as expected for a fast one-electron exchange system exhibiting an ideal Nernstian behavior: the peak current is proportional to the square root of the potential scan rate, the peak-to-peak potential separation is very close to the theoretical value of 59 mV and potential scan rate independent. Such a fast electron-transfer process of PIND-Ru-PIND is a desired feature for a successful design of an ECL system.

4.3. Intercalation with DNA

To determine the mode of interaction of PIND-Ru-PIND with ds-DNA, UV-vis spectrophotometry of PIND-Ru-PIND in the presence of increasing amounts of salmon sperm DNA was investigated. In the UV-vis spectrophotometry, hypochromism and red shift are signatures of intercalative binding where the fused planar aromatic ring system of a threading intercalator inserts itself between the base pairs of ds-DNA. As shown in Figure 5, the addition of DNA to PIND-Ru-PIND at a DNA base pair/PIND-Ru-PIND ratio of 5.0 resulted in a 45% decrease and a 3-nm-red-shift of the ND absorption band at 364 and 385 nm. Similar phenomena were previously observed with ND having aliphatic tertiary amine side chains (25). The hypochromism of the PIND absorption band reached a plateau at the base pair/PIND-Ru-PIND ratio ~7.0, and a constant hypochromism was observed for the ratio above this value. A single clean isosbestic point was observed at all DNA base pair/PIND-Ru-PIND ratios, suggesting that only one spectrally distinct PIND-Ru-IND/DNA complex is present. Both observations are qualitatively consistent with those observed for intercalating compounds, indicating that binding of PIND-Ru-PIND to ds-DNA takes place by preferential intercalation. In addition, after the PIND groups have

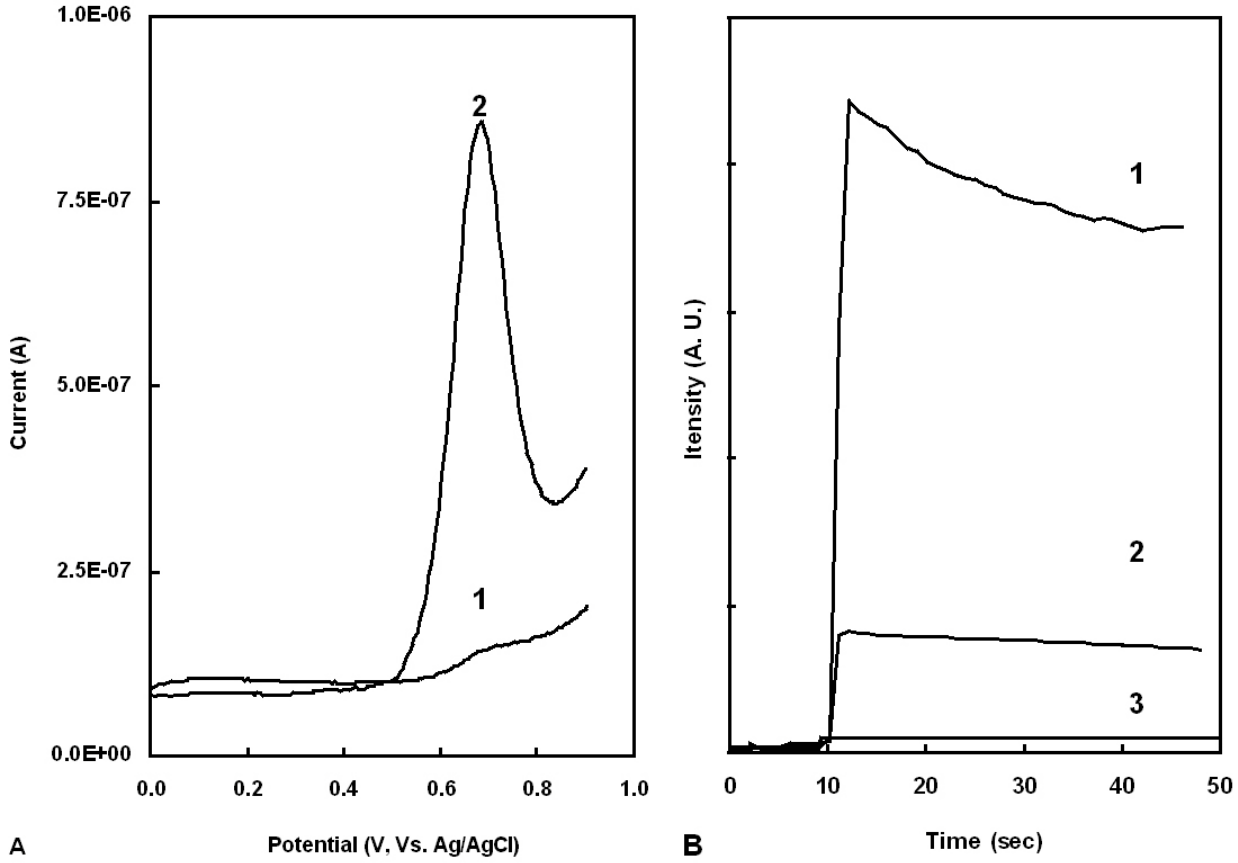

Figure 7. A. Linear scan voltammograms of PIND-Ru-PIND bound to (1) 1.0 μM non-complementary DNA, and to (2) 200 nM of complementary DNA hybridized biosensors. Supporting electrolyte pH 7.0 0.10 M phosphate buffer, potential scan rate 100 mV/s. B. ECL responses at 610 nm of PIND-Ru-PIND bound to (1) 1.0 nM non-complementary, (2) 50 pM one-base mismatched, and (3) 0 pM complementary DNA hybridized biosensor. Poise potential 1.0 V, pH 7.0 0.10 M phosphate saturated with TPA.

intercalated with ds-DNA, the dicationic $Ru(dmbpy)_2$ group in PIND-Ru-PIND forms an ion-pair with a phosphate of ds-DNA, making the two intercalated PIND groups more tightly fixed in between the base pairs of ds-DNA. A detail spectroscopic study of the intercalation is underway.

4.4. ECL behavior of PIND-Ru-PIND in TPA solution

The cyclic voltammetric and ECL responses of 5.0 μM PIND-Ru-PIND in pH 7.0 0.10 M phosphate buffer saturated with TPA co-reactant at a gold electrode are depicted in Figure 6. As shown in Figure 6A, the peak potential for the oxidation of TPA occurred at 1.0 V (Figure 6A trace 3) while that of PIND-Ru-PIND occurred at 0.68 V (Figure 6A trace 2), implying that the oxidation of PIND-Ru-PIND at the electrode surface occurs before that of TPA may be required for the production of ECL. The maximum ECL intensity for this system was observed at 0.94 V (Figure 6A trace 1). Figure 6B shows the ECL spectrum of PIND-Ru-PIND compared with its photoluminescence spectrum. As expected, within experimental error, the ECL spectra obtained for PIND-Ru-PIND at different positive potential biases have the same features as its photoluminescence spectrum in phosphate buffer. This is because the emission arises from the decay of the same MLCT excited state $Ru(dmbpy)_2^{2+*}$, generated by either illumination or electrochemical excitation.

4.5. Analytical applications of PIND-Ru-PIND in ultrasensitive DNA biosensors

DNA biosensors with redox active moieties grafted ND as electrochemical indicators have previously been reported (15, 26). When hybridization occurs, ND selectively interacts with the ds-DNA and gave a greatly enhanced analytical signal compared to non-hybridized ss-DNA. The difference in voltammetric peak current is used for quantitation purpose. However, to our knowledge, no study has been done on the ECL detection of DNA using threading intercalator. Similar to the redox active ND intercalator, PIND-Ru-PIND was firstly evaluated as an electroactive tag for possible applications in ultrasensitive DNA sensing. In the first hybridization test, a complementary and a non-complementary CP (control) coated biosensor were hybridized to the target DNA. Upon hybridization, the complementary target DNA was selectively bound to its complementary CP and became

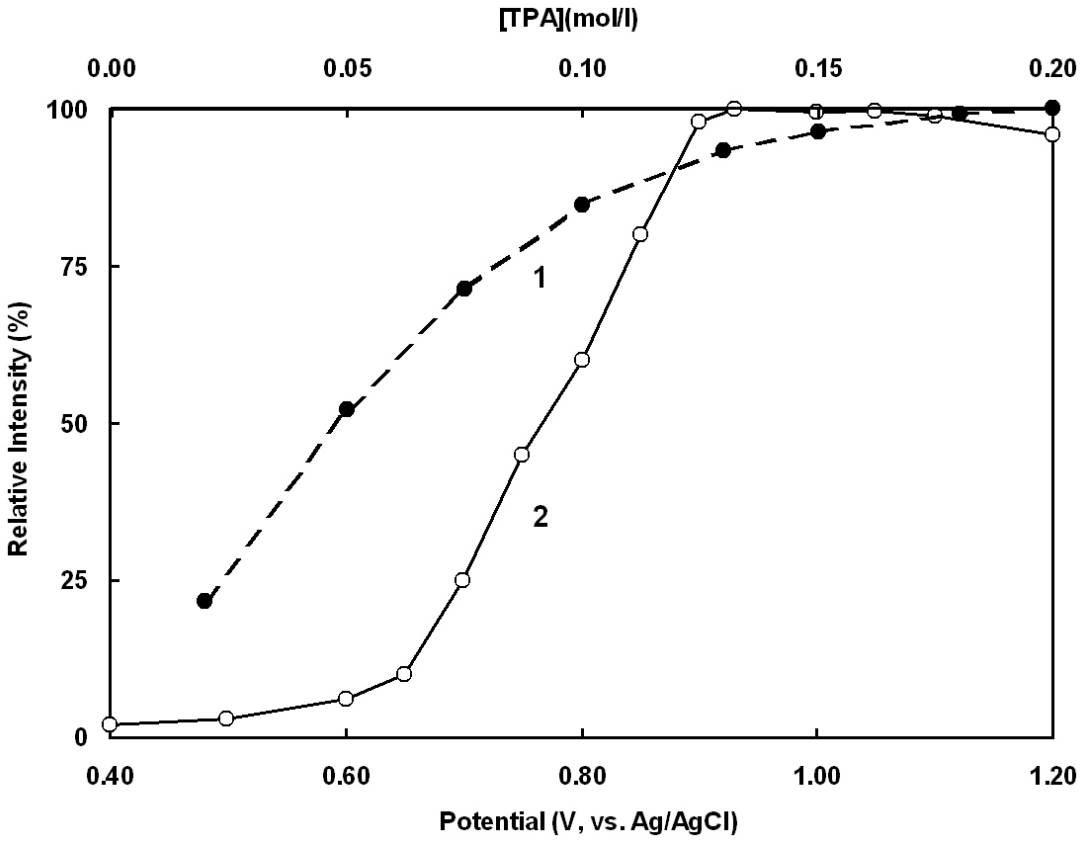

Figure 8. Effect of (1) TPA and (2) applied potential on the ECL responses at 610 nm of 50 pM complementary DNA after incubation in 10 μM PIND-Ru-PIND.

fixed on the biosensor surface. On the other hand, hybridization with the non-complementary CP failed to capture any of the target DNA, and therefore little change of the biosensor was expected. Thorough rinsing with the hybridization buffer washed off most of the non-hybridization related DNA. PIND-Ru-PIND was brought to the biosensor surface during a subsequent incubation with a PIND-Ru-PIND solution. Linear scan voltammograms for the biosensors after hybridization are shown in Figure 7A. For the non-complementary CP coated biosensor, after hybridization a minute voltammetric peak was observed at the redox potential of PIND-Ru-PIND (Figure 7A trace 1), largely due to pure electrostatic interaction of residual PIND-Ru-PIND and CP on the biosensor surface. As shown in trace 2, after hybridization with the complementary CP coated biosensor, a slight positive shift in the redox potential was observed and the peak current increased by as much as 100-fold. It was found that extensive washing with NaCl-saturated pH 7.0 0.10 M phosphate buffer removed most of the non-specific PIND-Ru-PIND uptake. These results clearly demonstrated that PIND-Ru-PIND selectively interacts with ds-DNA and the PIND-Ru-PIND–ds-DNA adduct has a very slow dissociation rate, which paves the way for developing ultrasensitive DNA biosensors. Consequently, using the intercalated PIND-Ru-PIND as the electroactive indicator for direct detection of DNA was evaluated. A dynamic range of 1.5 to 300 nM with a detection limit of 0.80 nM was obtained.

The ECL behavior of the hybridized biosensors before and after incubation with PIND-Ru-PIND were then examined with an positive potential bias of 1.0 V applied to the biosensors. Figure 7B shows ECL responses of various biosensors after hybridization with target DNAs and incubation with PIND-Ru-PIND. Very little ECL response was observed for the biosensor hybridized with the non-complementary target DNA, largely due to the presence of a very small amount of electrostatically bound PIND-Ru-PIND to the DNA. It can be seen that the presence of intercalated PIND-Ru-PIND in the complementary target DNA hybridized biosensor greatly increase the ECL signal of the system with an enhancement of ~50-fold. In contrast, no ECL signal was observed at the complementary DNA hybridized biosensor before PIND-Ru-PIND incubation. The much improved ECL response after PIND-Ru-PIND intercalation is indeed due to a genuine ECL process of the $Ru(dmpy)_2$ moieties (see above). The selectivity was evaluated at 50 pM by analyzing one-mismatched DNA under hybridization conditions set for the perfectly matched sequence. A ~65% drop in ECL intensity was observed, readily allowing discrimination between the perfectly matched and mismatched oligonucleotides. Figure 8 shows the effect of TPA and applied potential on the ECL signal of a 50 pM complementary DNA hybridized biosensor. The optimum concentration of TPA is ~0.20 M (saturated). This is readily explained because at lower TPA concentration,

the electron-transfer reaction between activated PIND-Ru-PIND and an intermediate in the oxidation of TPA is less effective. To maximize ECL sensitivity, ECL measurements were always conducted in the saturated TPA solution. Variation of the applied potential had a profound effect on the ECL intensity (Figure 8 trace 2). The threshold potential of ECL was found to be 0.65 V and the ECL signal increased rapidly beyond the threshold potential until a maximum intensity was reached in the range of 0.93–1.05 V. Under the optimized conditions, the ECL signal was proportional to the target DNA concentration in the range of 0.70–400 pM with a detection limit of 400 fM, 2000-fold higher that of the direct voltammetric detection of DNA. The ECL data agreed well with the voltammetric results obtained earlier in solution and confirmed again that PIND-Ru-PIND is electrochemiluminescent and it can be used to detect DNA with high specificity and sensitivity.

5. CONCLUSIONS

An ECL DNA threading bis-intercalator, PIND-Ru-PIND, was synthesized and characterized. Spectrometric and electrochemical characterization confirmed the formation of the desired compound. Successful attempts were made in utilizing PIND-Ru-PIND as an effective redox active and ECL tag in non-labeling DNA assays. The proposed biosensor promises to greatly improve the practicability of ECL detection approaches due to the use of non-labeling procedure. The combination of the selective intercalation to ds-DNA with ECL of PIND-Ru-PIND provides a simple, direct, and highly sensitive non-labeling method for DNA quantification. We believe this method could have a wide applicability to ultrasensitive DNA assays. The flexibility of non-labeling allows for the fast and easy operation of the biosensor/biosensor array.

6. ACKNOWLEDGEMENT

The authors would like to acknowledge financial support from IBN/A*STAR.

7. REFERENCES

1. J. Wang: SURVEY AND SUMMARY: From DNA biosensors to gene chips. *Nucleic Acids Res* 28, 3011–3016 (2000)

2. T.G. Drummond, M.G. Hill & J.K. Barton: Electrochemical DNA sensors. *Nat Biotechnol* 21, 1192–1196 (2003)

3. E. Palecek & F. Jelen: Electrochemistry of nucleic acids and development of DNA sensors. *Crit Rev Anal Chem* 3, 261–270 (2002)

4. G. Sutherland & J. Mulley: In: Nucleic Acid Probes. Ed: R.H. Symons. CRC Press, Boca Raton, FL, 159–201 (1989)

5. L.J. Kricka: Nonisotopic Probing, Blotting and Sequencing. 2nd Ed, Academic Press Inc, San Diego, CA (1995)

6. (a) W. Miao and A.J. Bard: Electrogenerated chemiluminescence. 72. Determination of immobilized DNA and C-Reactive Protein on Au(111) electrodes using Tris(2,2'-bipyridyl)ruthenium(II) labels. *Anal Chem* 75, 5825–5834 (2003); (b) W. Miao and A.J. Bard:. Electrogenerated chemiluminescence. 77. DNA hybridization detection at high amplification with $[Ru(bpy)_3]^{2+}$-containing microspheres. *Anal Chem* 76, 5379–538 (2004); (c) W. Miao and A.J. Bard: Electrogenerated chemiluminescence. 80. C-Reactive Protein determination at high amplification with $[Ru(bpy)_3]^{2+}$-containing microspheres. *Anal Chem* 76, 7109–7113 (2004); (d) X-H, Xu, H.C. Yang, T.E. Mallouk and A.J. Bard: Immobilization of DNA on an aluminum(III) alkanebisphosphonate thin film with electrogenerated chemiluminescent detection. *J Am Chem Soc* 116, 8386–8387 (1994)

7. T.J. Meyer: Chemical approaches to artificial photosynthesis. *Acc Chem Res* 22, 163–170 (1989)

8. J.V. Caspar and T.J. Meyer: Photochemistry of tris(2,2'-bipyridine)ruthenium(2+) ion ($Ru(bpy)_3^{2+}$). solvent effects. *J Am Chem Soc* 105, 5583–5590 (1983)

9. J.V. Houten and R.J. Watts: Temperature dependence of the photophysical and photochemical properties of the tris(2,2'-bipyridyl)ruthenium(II) ion in aqueous solution. *J Am Chem Soc* 98, 4853–4858 (1976)

10. N.E. Tokel and A.J. Bard: Electrogenerated chemiluminescence. IX. Electrochemistry and emission from systems containing tris(2,2'-bipyridine)ruthenium(II) dichloride. *J Am Chem Soc* 94, 2862–2866 (1972)

11. K. Hashimoto, K. Itoand Y. Ishimori: Sequence-Specific gene detection with a gold electrode modified with DNA probes and an electrochemically active dye. *Anal Chem* 66, 3830–3833 (1994)

12. M.T. Carter, M. Rodriguez and A.J. Bard: Voltammetric studies of the interaction of metal chelates with DNA. 2. Tris-chelated complexes of cobalt(III) and iron(II) with 1,10-phenanthroline and 2,2'-bipyridine. *J Am Chem Soc* 111, 8901–8911 (1989)

13. S.M. Zeman, D.R. Phillips & D.M. Crothers: Characterization of covalent Adriamycin-DNA adducts. *Proc Natl Acad Sci USA* 95, 11561–11565 (1998)

14. K.E. Erkkila, D.T. Odom and J.K. Barton: Recognition and reaction of metallointercalators with DNA. *Chem Rev* 99, 2777–2795 (1999)

15. N.C. Tansil, H. Xie, F. Xie and Z. Gao: Direct detection of DNA with an electrocatalytic threading intercalator. *Anal Chem* 77, 126–134 (2005)

16. (a) A. Mugweru, B. Wang and J. Rusling: Voltammetric sensor for oxidized DNA using ultrathin films of Osmium and Ruthenium metallopolymers. *Anal Chem* 76, 5557–5563 (2004); (b) L. Dennany, R.J. Forster and J.F. Rusling: Simultaneous direct electrochemiluminescence and catalytic voltammetry detection of DNA in ultrathin films. *J Am Chem Soc* 125, 5213–5218 (2003)

17. P. A. Lay, A. M. Sargeson & H. Taube: cis-Bis(2,2'-bipyridine-N, N') complexes of ruthenium (III)/(II) and Osmium (III)/(II). *Inorg Synth* 24, 291-299 (1986)

18. A. Rademacher, S. Maerkle & H. Ianghals: *Chem Ber* 115, 2972–2976 (1982)

19. H.E. Katz, J. Johnson, A.J. Lovinger and W. Li: Naphthalenetetracarboxylic diimide-based n-channel

transistor semiconductors: structural variation and thiol-enhanced gold contacts. *J Am Chem Soc* 122, 7787–7792 (2000)
20. (a) H. Xie, C. Zhang and Z. Gao: Amperometric detection of nucleic acid at femtomolar levels with a nucleic acid/electrochemical activator bilayer on gold electrode. *Anal Chem* 76, 1611–1617 (2004); (b) H. Xie, Y.H. Yu, F. Xie, Y.Z. Lao and Z. Gao: A nucleic acid biosensor for gene expression analysis in nanograms of mRNA. *Anal Chem* 76, 4023–4029 (2004); (c) H. Xie, Y. H. Yu, P. L. Mao and Z. Gao: Highly sensitive amperometric detection of genomic DNA in animal tissues. *Nucleic Acids Res* 32, e15 (2004)
21. A.B. Steel, M.T. Herne & M.J. Tarlov: Electrochemical quantitation of DNA immobilized on gold. *Anal Chem* 70, 4670–4677 (1998)
22. A. Juris, V. Balzani, F. Barigelletti, S. Campagna. P. Belser and A. von Zelewsky: Ru(II) polypyridine complexes: photophysics, photochemistry, eletrochemistry, and chemiluminescence . *Coord Chem Rev* 84, 85–277 (1988)
23. S. F. Yen, E.J. Gabbay & W.D.Wilson: Interaction of aromatic imides with DNA. 1. Spectrophotometric and viscometric studies. *Biochemistry* 21, 2070–2076(1982)
24. D.W. Dixon, N.B. Thornton, V. Steullet &T. Netzel: Effect of DNA scaffolding on intramolecular electron transfer quenching of a photoexcited Ruthenium(II) polypyridine naphthalene diimide . *Inorg Chem* 38, 5526–5534 (1999)
25. (a) R.S. Lokey, Y. Kwok, V. Guelev, C.J. Pursell, L.H. Hurley & B.L.Iverson: A new class of polyintercalating molecules. *J Am Chem Soc* 119, 7202–7210 (1997); (b) M.M. Murr, M.T. Harting, V. Guelev, J. Ren, J.B. Chaires & B.L. Iverson: An octakis-intercalating molecule . *Bioorg. Med. Chem.* 2001, 9, 1141–1148.
26. S. Takenaka, K. Yamashita, M. Takagi, Y. Uto & H. Kondo: DNA sensing on a DNA probe-modified electrode using ferrocenylnaphthalene diimide as the electrochemically active ligand . *Anal Chem* 72, 1334–1341 (2000)

Key Words: Electrochemiluminescence, Threading Intercalator, DNA Biosensor

Send correspondence to: Dr Zhiqiang Gao Institute of Bioengineering and Nanotechnology, 31 Biopolis Way, Singapore 138669, Tel: 6824-7113, Fax: 6478-9084, E-mail: zqgao@ibn.a-star.edu.sg